R & M No.3830

R &M No.3830

PROCUREMENT EXECUTIVE, MINISTRY OF DEFENCE

Aeronautical Research Council
Reports and Memoranda

THE AERODYNAMIC NOISE OF A SLOT IN AN AEROFOIL

by

M.S. Howe

Engineering Department, Cambridge

London: Her Majesty's Stationery Office
1978

PRICE £5 NET

THE AERODYNAMIC NOISE OF A SLOT IN AN AEROFOIL

by M. S. Howe*

Engineering Department, Cambridge

Reports and Memoranda No.3830**

August 1977

SUMMARY

This Report describes a theoretical investigation of the noise generated when turbulence interacts with a slot between a wing and flap. The slot is modelled by the region between two overlapping, semi-infinite rigid planes representing the wing and flap, and sound is produced when turbulence convects above, below or through the slot. The analysis determines the dependence of the radiated sound on the characteristic turbulence velocity, the effect of forward flight on the field shape, and properties of the field radiated to the side of the aircraft flight path.

---

* Vacation consultant, summer 1976

** Replaces RAE Technical Report 77129 - ARC 37794

LIST OF CONTENTS

1 INTRODUCTION

It has been recognized for some time (Gibson, 1972, 1973, 1974) that consequent to the progressive introduction of relatively quiet engines the non-propulsive or airframe noise of a large subsonic aircraft will constitute an increasingly significant proportion of the total radiated sound. Airframe noise is not particularly important for an aerodynamically clean aircraft (*ie* one with undercarriage and high-lift devices retracted), but as this represents a basic flight configuration it has nonetheless stimulated both theoretical and experimental studies (Gibson 1972, Morgan & Hardin 1974, Healy 1974, Hardin 1976). Under these conditions the principal component of airframe noise appears to be associated with the convection of turbulent eddies past the wing trailing edge. Deployment of either undercarriage or of high-lift devices, such as flaps, increases the airframe sound pressure level by about 8 dB for an aircraft such as the VC 10 (Fethney, 1975) with still larger increases at the lower frequencies (below about 250 Hz on the VC 10).

It can be argued that an important component of the noise generated by a flap results from the interaction between turbulent eddies in the boundary layer on the upper surface of the wing and the slot ahead of the flap nose. This is because the velocity over the upper surface at the slot is greater there than at the trailing edge of the flap. In order to determine the properties of the sound generated in this way an idealized problem is investigated in this Report in which the wing and flap are modelled by two overlapping semi-infinite rigid planes. The analysis is therefore concerned primarily with acoustic frequencies for which the wavelength does not exceed the chord of the flap. Within the limits of this constraint the discussion is directed at estimating the effective source type (monopole, dipole, etc) of slot noise, together with its dependence on the flight velocity of the aircraft and the characteristics of the turbulence.

The idealized configuration of the wing/flap system is defined in section 2, and the general aerodynamic sound problem is formulated and solved in terms of analytical results derived in the Appendix. These general conclusions are particularized in sections 3 and 4 by the consideration of a specific model of the turbulent flow inhomogeneities in the boundary layer of the airfoil. The results obtained in this way are used (section 5) to determine: (i) the effect of forward flight on the acoustic field shape; (ii) the velocity dependence of the aerodynamic sound; (iii) the characteristics of the sound radiated to the side of the flight path.

The principal conclusions are summarized in section 6.

2 THEORETICAL MODEL OF THE GENERATION OF SOUND BY THE INTERACTION OF TURBULENCE WITH A SLOT

The idealized geometry of the wing/flap configuration is depicted in Fig 1, and consists of two parallel, overlapping semi-infinite rigid planes. Fig 1a views the system from beneath the aircraft; the upper and lower half-planes model respectively the wing and flap, the region of overlap AB constituting the slot. Coordinate axes (x_1,x_2,x_3) are taken with origin at a point 0 which lies in the wing in the plane of the leading mouth A of the slot, the positive x_1 -axis being in the flight direction, x_2 vertically downwards and x_3 parallel to the leading and trailing edges of the slot. The slot has length ℓ in the streamwise direction, width h in the perpendicular or x_2 -direction and is of infinite span. Accordingly the wing and flap occupy respectively the regions $(-\ell < x_1 < \infty\ ,\ x_2 = 0\ ,\ -\infty < x_3 < \infty)$ and $(-\infty < x_1 < 0\ ,\ x_2 = h\ ,\ -\infty < x_3 < \infty)$. We shall be considering the interaction between the slot and incident compact turbulent eddies, or boundary layer disturbances leading to vortex shedding, and the approximation of infinite wing-span should be adequate provided that the interaction occurs at distances from the wing tip or the fuselage which exceed the characteristic acoustic wavelength. Similarly in modelling the flap by a semi-infinite rigid plane the discussion is limited to that range of frequencies for which the wavelength is smaller than the flap chord.

In the undisturbed state the fluid will be assumed to have uniform thermodynamic properties and a mean velocity U relative to the aerofoil in the negative x_1 -direction, corresponding to forward flight of the aircraft at speed U . Let c denote the speed of sound, then we shall suppose also that the Mach number $M = U/c$ is in the low subsonic range. Specifically the analysis to be described requires that

$$\frac{\omega h}{c}\Big/\sqrt{1 - M^2} \ll 1\ , \tag{2-1}$$

where ω is the characteristic radian frequency (relative to the aerofoil) of the sound. In other words the width h of the slot must be small compared with the acoustic wavelength, and the Mach number M should not exceed about 0.5. No restriction is placed on the length ℓ of the slot.

Sound is generated by the unsteady motion induced in the slot when a boundary layer disturbance is swept through or past either of the mouths A, B. The strength and field shape of the radiation will be estimated on the basis of linearized unsteady aerodynamics, in a manner analogous to classical thin aerofoil theory (von Kármán and Sears 1938). The total enthalpy is defined by

$$B = w + \tfrac{1}{2}\underset{\sim}{v}^2 \tag{2-2}$$

$\underset{\sim}{v}$ being the velocity, and where w is the specific enthalpy of the fluid which is constant throughout the steady flow which exists in the absence of the incident eddy, provided that the mean flow is isentropic. The linearized equation determining the fluctuations in B produced by unsteady distributions of vorticity has been derived by Howe (1976), and has the form

$$\left\{ \frac{1}{c^2}\left(\frac{\partial}{\partial t} - U\frac{\partial}{\partial x_1} \right)^2 - \nabla^2 \right\} B = - U_s \operatorname{div} (\underset{\sim}{\omega} \wedge \underset{\sim}{i}) \tag{2-3}$$

where $\underset{\sim}{i}$ is a unit vector parallel to the x_1-axis, $\underset{\sim}{\omega}$ is the vorticity and U_s is the eddy convection velocity (in the negative x_1-direction) which is assumed to be constant. The magnitude of U_s is determined by the characteristics of the turbulent boundary layer in which the eddy is convected, and is typically of order $0.8U$.

The turbulence is assumed to be effectively frozen during the period in which a significant interaction occurs:

$$\underset{\sim}{\omega} \equiv \underset{\sim}{\omega}(x_1 + U_s t, x_2, x_3) \tag{2-4}$$

although the convection velocity U_s may vary from eddy to eddy.

The inhomogeneous wave equation (2-3) may be solved once the appropriate Green's function $G(\underset{\sim}{x},\underset{\sim}{y},t,\tau)$ has been found. This is the 'advanced potential' solution of

$$\left\{ \frac{1}{c^2}\left(\frac{\partial}{\partial \tau} - U\frac{\partial}{\partial y_1} \right)^2 - \frac{\partial^2}{\partial y_j^2} \right\} G = \delta(\underset{\sim}{x} - \underset{\sim}{y})\delta(t - \tau) \tag{2-5}$$

which satisfies the condition of vanishing normal derivative on the rigid surfaces and corresponds to an implosive sink at the point $\underset{\sim}{x}$ at time t which is zero for $\tau > t$. The form of $G(\underset{\sim}{x},\underset{\sim}{y},t,\tau)$ is determined in the Appendix in the particular case in which the compactness condition (2-1) is satisfied.

It may then be shown by means of a well known procedure (see, *eg*, Stratton 1941, Chapter 8) that the fluctuation in the stagnation enthalpy B due to the interaction of the turbulence with the slot is given by the convolution product

$$B(\underset{\sim}{x},t) = -U_s \int G(\underset{\sim}{x},\underset{\sim}{y},t,\tau) \frac{\partial}{\partial \underset{\sim}{y}} \cdot (\underset{\sim}{\omega} \wedge \underset{\sim}{i})(\underset{\sim}{y},\tau) d^3\underset{\sim}{y} d\tau$$

$$+ \oint G(\underset{\sim}{x},\underset{\sim}{y},t,\tau)\underset{\sim}{n} \cdot \frac{\partial B}{\partial \underset{\sim}{y}} (\underset{\sim}{y},\tau) d^2\underset{\sim}{y} d\tau \quad . \tag{2-6}$$

The second integral is taken over the rigid surfaces of the slot for which $\underset{\sim}{n}$ is the unit outward normal. Applying the divergence theorem to the volume integral we have:

$$B(\underset{\sim}{x},t) = U_s \int (\underset{\sim}{\omega} \wedge \underset{\sim}{i})(\underset{\sim}{y},\tau) \cdot \frac{\partial G}{\partial \underset{\sim}{y}} (\underset{\sim}{x},\underset{\sim}{y},t,\tau) d^3\underset{\sim}{y} d\tau$$

$$+ \oint G(\underset{\sim}{x},\underset{\sim}{y},t,\tau)\underset{\sim}{n} \cdot \left\{ \frac{\partial B}{\partial \underset{\sim}{y}} - U_s \underset{\sim}{\omega} \wedge \underset{\sim}{i} \right\} (\underset{\sim}{y},\tau) d^2\underset{\sim}{y} d\tau \quad . \tag{2-7}$$

For the assumed isentropic flow, the perturbation momentum equation is

$$\frac{\partial \underset{\sim}{v}}{\partial t} = -\nabla B + U_s \underset{\sim}{\omega} \wedge \underset{\sim}{i} \quad . \tag{2-8}$$

It follows that the surface integral in (2-7) vanishes identically because $\underset{\sim}{n} \cdot \partial \underset{\sim}{v}/\partial t = 0$. Hence we have finally

$$B(\underset{\sim}{x},t) = U_s \int (\underset{\sim}{\omega} \wedge \underset{\sim}{i})(\underset{\sim}{y},\tau) \cdot \frac{\partial G}{\partial \underset{\sim}{y}} (\underset{\sim}{x},\underset{\sim}{y},t,\tau) d^3\underset{\sim}{y} d\tau \quad . \tag{2-9}$$

In this result the coordinate system $\underset{\sim}{x}$ is fixed relative to the wing/flap system, and therefore a fixed observer location $\underset{\sim}{x}$ translates at the flight velocity U relative to the ground. For a stationary observer it is convenient to adopt a far field representation in which the observer position is specified relative to the aircraft at the time of emission of the sound. Let (r,θ,ϕ) be the spherical polar coordinates of the observer in this reference frame, the polar angle θ being measured from the positive x_1 -direction. The following equations relate the new and the old coordinate systems

$$\left.\begin{aligned} x_1 &= r(\cos\theta - M) \\ x_2 &= r \sin\theta \cos\phi \\ x_3 - y_3 &= r \sin\theta \sin\phi \quad . \end{aligned}\right\} \tag{2-10}$$

In this new frame of reference the phase of the radiated sound is proportional to $t - r/c$ in the far field. Also $B(\underset{\sim}{x},t)$ is related to the velocity potential ϕ, say, by $B = -\partial\phi(\underset{\sim}{x},t)/\partial t$. Hence at a far field point the acoustic pressure p is given by

$$\left.\begin{aligned} \frac{p}{\rho_0} &= -\left(\frac{\partial}{\partial t} - U\frac{\partial}{\partial x_1}\right)\phi \\ &\simeq B\left(1 + M\frac{\partial r}{\partial x_1}\right) \\ &= \frac{B}{1 - M\cos\theta} \end{aligned}\right\} \qquad (2\text{-}11)$$

where ρ_0 is the mean density, and (2-9) implies that

$$\frac{p(\underset{\sim}{r},t)}{\rho_0} = \frac{U_s}{1 - M\cos\theta}\int (\underset{\sim}{\omega} \wedge \underset{\sim}{i})(\underset{\sim}{y},\tau) \cdot \frac{\partial G}{\partial \underset{\sim}{y}}(\underset{\sim}{r},\underset{\sim}{y},t,\tau)\,d^3\underset{\sim}{y}\,d\tau \qquad (2\text{-}12)$$

$\underset{\sim}{r}$ being the retarded observer position (r,θ,ϕ).

3 THE MECHANISM OF VORTEX SOUND

Let $\underset{\sim}{\omega} = (\omega_1,\omega_2,\omega_3)$ be the (x_1,x_2,x_3) components of the incident vorticity distribution. The integrand of (2-12) then has the explicit form

$$\omega_3\frac{\partial G}{\partial y_2} - \omega_2\frac{\partial G}{\partial y_3}$$

In the Appendix it is shown that for the frozen distribution of vorticity (2-4) the second term in this expression makes a negligible contribution to the radiated sound. The remaining term involves the component ω_3 of the vorticity which is parallel to the leading and trailing edges of the slot. Tracing back the analysis of section 2 to the inhomogeneous wave equation (2-3) we see that the effective aerodynamic 'source' is therefore $-\partial(\omega_3 U_s)/\partial y_2$, a dipole orientated perpendicular to the wing/flap system, and the integral expression (2-12) for the radiated sound reduces to

$$\frac{p(\underset{\sim}{r},t)}{\rho_0} = \frac{U_s}{(1 - M\cos\theta)}\int \omega_3(\underset{\sim}{y},\tau)\frac{\partial G}{\partial y_2}(\underset{\sim}{r},\underset{\sim}{y},t,\tau)\,d^3\underset{\sim}{y}\,d\tau \quad . \qquad (3\text{-}1)$$

Consider the low frequency case in which the wavelength of the generated sound greatly exceeds the length ℓ of the slot. In this case the Green's function G possesses a simplified form essentially because the slot does not have a resonant response. Thus, in particular, when the compact incident eddy straddles the x_1 -axis and is located near the leading edge A of the slot it is shown in the Appendix (equation (A-38)), that

$$G(\underset{\sim}{r},\underset{\sim}{y},t,\tau) = \frac{h\sqrt{1 - M^2}}{2\pi^2 \ell r(1 - M\cos\theta)} \phi_1^*(\underset{\sim}{Y})\delta(t - \tau - r/c) \qquad (3\text{-}2)$$

where the observer is located in the far field *below* the wing/flap system ($x_2 > 0$). The vector $\underset{\sim}{Y}$ is related to $\underset{\sim}{y}$ by the Prandtl-Glauert transformation

$$Y = (Y_1, Y_2) \equiv \left(\frac{y_1}{\sqrt{1 - M^2}}, y_2\right) \qquad (3\text{-}3)$$

and the function $\phi_1^*(\underset{\sim}{Y})$ is the real part of the complex potential

$$w_1(z) = \phi_1^*(\underset{\sim}{Y}) + i\psi_1^*(\underset{\sim}{Y}) \quad . \qquad (3\text{-}4)$$

In this expression $z = Y_1 + iY_2$, and $w_1(z)$ characterises a two-dimensional reciprocating flow in planes of constant x_3 in the mouth A of the slot. Note that (3-2) depends on the y_3 -source position coordinate only insofar as it enters the retarded distance r between source and observer.

Using (3-2) in the integral expression (3-1) for the far field sound we have:

$$\frac{p(\underset{\sim}{r},t)}{\rho_0} \simeq \frac{h\sqrt{1 - M^2}}{2\pi^2 \ell r(1 - M\cos\theta)^2} \int U_s \omega_3(y_1 + U_s\tau, y_2, y_3) \times$$

$$\times \frac{\partial \phi_1^*}{\partial y_2}(\underset{\sim}{Y})\delta\left(t - \tau - \frac{r}{c}\right) d^3\underset{\sim}{y}d\tau \ , \qquad (3\text{-}5)$$

ie, from (3-4) and the Cauchy-Riemann equations

$$\frac{p(\underset{\sim}{r},t)}{\rho_0} = \frac{h(1 - M^2)}{2\pi^2 \ell r(1 - M\cos\theta)^2} \int \left[\omega_3 \frac{D\psi_1^*}{Dt}\right] d^3\underset{\sim}{y} \ , \qquad (3\text{-}6)$$

where the term in square brackets is evaluated at the retarded time $t - r/c$. The material derivative $D/Dt = \partial/\partial t - U_s \partial/\partial x_1$ where U_s is the local mean flow velocity in the turbulent boundary layer. The stream function $\psi_1^*(\underset{\sim}{Y})$ is dimensionless (see equation (A-14)), and (3-6) therefore indicates that the far field sound pressure level scales on the fourth power of the characteristic velocity U_s . Forward motion of the aircraft amplifies the SPL by four powers of the Doppler factor $(1 - M \cos \theta)^{-1}$. Both of these attributes are characteristic of a *monopole* source which may be ascribed to the unsteady 'sloshing' of fluid through the slot produced by the passage of the eddy.

A simpler representation of the acoustic field is obtained for a 'horseshoe' eddy for which the vortex lines terminate deep within the laminar sub-boundary layer of the wing, say. The dominant contribution to ω_3 , the transverse component of vorticity, then occurs principally in the outer or turbulent region of the boundary layer flow. In a first approximation it may be assumed that

$$\omega_3 = \Gamma \delta(x_1 + U_s t)\delta(x_2 - d)H(\Lambda - 2|x_3|) \qquad (3\text{-}7)$$

where $H(x)$ is the Heaviside unit function, *ie*, the x_3 -component of vorticity is modelled by a concentrated line vortex of strength Γ and length Λ which convects perpendicular to itself in the streamwise direction at a constant distance d from the underside of the wing.

In this case (3-5) reduces to

$$\frac{p(\underset{\sim}{r},t)}{\rho_0} = \frac{\Gamma}{2\pi^2}\left(\frac{h\Lambda}{\ell r}\right)\frac{(1 - M^2)}{(1 - M \cos \theta)^2}\left[\frac{D\psi_1^*}{Dt}\right] , \qquad (3\text{-}8)$$

where the term in square brackets is evaluated at the retarded position of the vortex. The function $\psi_1^*(\underset{\sim}{Y})$ is constant along the streamlines of a two-dimensional potential flow into the mouth A of the slot from a fluid that has zero velocity at infinity. The result (3-8) accordingly demonstrates that the intensity of the radiated sound is determined by the rate at which the vortex cuts across the streamlines of such a hypothetical flow. The streamlines $\psi_1^* = \text{constant}$ are densely spaced transverse to the mean flow direction close to the sharp edges of the slot (Fig 2) which are therefore the most acoustically sensitive regions of the flow.

4 SOUND GENERATION BY A HARMONIC EDDY

When the characteristic wavelength of the sound is not large compared with the length ℓ of the slot the Green's function $G(\underset{\sim}{x},\underset{\sim}{y},t,\tau)$ ceases to assume the relatively simple form shown in equation (3-2). The appropriate expressions for G are given by equations (A-36) and (A-39) of the Appendix respectively for the cases in which the aerodynamic source is located well within an acoustic wavelength of the mouth A or the trailing edge B of the slot.

In order to examine the generation of sound in this more general situation it is convenient to modify the discrete model (3-7) of the transverse component ω_3 of the eddy vorticity by writing:

$$\omega_3 \equiv \omega_3(x_1 + U_s t, x_2, x_3)$$

$$= H(\Lambda - 2|x_3|) \sum_{\Omega} \delta(x_2 - d) V(\Omega) e^{-i\Omega(t+x_1/U_s)} \quad . \tag{4-1}$$

This is a harmonic representation of a distribution of transverse vorticity which propagates at speed U_s in the plane $x_2 = d$ in the negative x_1-direction, and of which (3-7) is a special case. The characteristic turbulent fluctuation velocity $v(\Omega)$ is associated with the radian frequency Ω relative to the aerofoil, or eddy wavenumber $\kappa = \Omega/U_s$.

Consider the sound generated by a single component of (4-1), *ie*, take

$$\omega_3 = v\delta(y_2 - d) H(\Lambda - 2|y_3|) e^{-i\Omega(\tau+y_1/U_s)} \tag{4-2}$$

in the integral (3-1) for the acoustic pressure field. There are three cases to be distinguished:

(I) $d > h$, the incident eddy passes below the wing and flap:

(II) $0 < d < h$ the eddy convects through the slot:

(III) $d < 0$ the eddy passes above the wing.

Case I: $d > h$, eddy passes below the wing and flap.

The eddy interacts only with the leading portion A of the slot and the corresponding expression for the Green's function is given by equation (A-36) of the Appendix. Substituting this and (4-2) into the convolution integral (3-1) we obtain

$$\frac{p(\underset{\sim}{r},t)}{\rho_0} = \frac{U_s v}{4\pi^2}\left(\frac{h}{r}\right)\left(\frac{\Omega\Lambda}{c}\right)\frac{\sin\bar{\theta}}{(1 - M\cos\theta)^2}\, e^{-i\Omega(t-r/c)} \times$$

$$\times \left\{ \frac{I_1\left(\kappa\sqrt{1 - M^2}\right)\cos\left[\dfrac{\Omega\ell\sin\bar{\theta}}{c(1 - M^2)}\right]}{\sin\left[\dfrac{\Omega\ell\sin\bar{\theta}}{c(1 - M^2)} - \Delta(\Omega)\right]} - iI_2\left(\kappa\sqrt{1 - M^2}\right)\cos\Theta \right\} \quad \ldots (4\text{-}3)$$

where the observer position $\underset{\sim}{r}$ is below the wing/flap system. The various terms appearing in this expression are defined as follows:

(i) $\bar{\theta}$ is the angle between the x_3-axis (*ie* the transverse edge of the slot) and the 'Prandtl-Glauert stretched' observer position vector (X_1, X_2, x_3) defined by (3-3).

(ii)
$$\cos\Theta = \frac{X_1}{\sqrt{X_1^2 + X_2^2}} .$$

Both of these quantities can be expressed in terms of the coordinates (r,θ,ϕ) of the retarded position of the observer, and the precise expressions together with other useful transformation formulae, are listed in the Table of the Appendix. The function $\Delta(\Omega)$ is a complex valued quantity which limits the response of the slot when it is excited at one of its resonant frequencies $\Omega \equiv \Omega(\bar{\theta})$ given by $\Omega\ell \sin\bar{\theta}/c(1 - M^2) = n\pi$ (n integral). It characterises the loss of energy from the oscillatory motion within the slot due to the radiation of sound from the mouths at A and B, and is given by equations (A-30) and (A-35) of the Appendix. In this respect it should be observed that the effective resonant frequency $\Omega(\bar{\theta})$ is a function of the length ℓ of the slot, the flight Mach number M and the angle $\bar{\theta}$, and in particular $\Omega(\bar{\theta})$ increases as the observer moves from a location directly beneath the flight path into a sideline direction.

In the 'flyover' plane ($\phi = 0$) beneath the aircraft it follows from the Table of the Appendix that $\sin\bar{\theta} = 1$; also if the flight velocity M is small $\cos\Theta \simeq \cos\theta$. In this case, therefore, the radiated sound given by (4-3) comprises an omnidirectional monopole together with a dipole whose axis is

orientated *parallel* to the mean flow through the slot. Forward flight of the aircraft at a non-negligible Mach number M modifies the structure of the field shape both by the appearance of Doppler factors $(1 - M \cos \theta)^{-1}$ and also because of the dependence of the angles $\bar{\theta}$ and Θ on M . These effects will be examined in more detail in section 5.

$$I_1\left(\kappa\sqrt{1 - M^2}\right), \quad I_2\left(\kappa\sqrt{1 - M^2}\right)$$

are the following integrals taken along the trajectory $y_2 = d$ of the incident transverse component of vorticity:

$$I_j = \int_{-\infty}^{\infty} \left(\frac{\partial \phi_j}{\partial Y_2}(\underset{\sim}{Y})\right)_{Y_2=d} e^{-i\kappa Y_1\sqrt{1-M^2}} dY_1, \quad (j = 1,2) . \qquad (4\text{-}4)$$

The functions $\phi_j^*(\underset{\sim}{Y})$ are the real parts of complex potentials $w_j(z)$ $(z = Y_1 + iY_2)$ defined implicitly by equations (A-14), (A-16) of the Appendix. The case $j = 1$ has already been encountered in the previous section, and defines a hypothetical potential flow into the mouth A of the slot; $j = 2$ corresponds to a streaming flow past the slot which does not penetrate more than a distance h or so within the mouth A and is parallel to the x_1-axis at great distances from A on the underside of the wing/flap system. The implicit representations (A-14) and (A-16) can be used to evaluate the Fourier integrals (4-4) as follows.

With $z = Y_1 + iY_2$ we have from the above

$$\frac{\partial \phi_j^*}{\partial Y_2} = \frac{i}{2}\left\{w_j'(z) - \overline{w_j'(z)}\right\} \qquad (4\text{-}5)$$

where the overbar and prime denote respectively the complex conjugate and differentiation with respect to z . Thus we can write

$$I_j = I_{j1} + I_{j2} \qquad (4\text{-}6)$$

where

$$\left.\begin{aligned} I_{j1} &= \frac{i}{2}\int_C w_j'(z)e^{-i\bar{\kappa}z}dz\,e^{-\bar{\kappa}d} \\ \overline{I_{j2}} &= \frac{i}{2}\int_C w_j'(z)e^{i\bar{\kappa}z}dz\,e^{\bar{\kappa}d} \end{aligned}\right\} \qquad (4\text{-}7)$$

the contour of integration C is $\mathrm{Im}\, z = d$ $(-\infty < \mathrm{Re}\, z < \infty)$ and we have set

$$\bar{\kappa} = \kappa\sqrt{1 - M^2} \quad . \qquad (4\text{-}8)$$

Consider in particular the evaluation of I_{11} . The function $w_1(z)$ is regular except for a branch cut coinciding with the flap $(-\infty < \mathrm{Re}\, z < 0$, $\mathrm{Im}\, z = h)$. Hence, since in the present case $d > h$, it follows that for $\bar{\kappa} < 0$ the integration contour in the z-plane can be displaced to $z = +i\infty$ where the integrand is exponentially small. Thus there is a non-trivial contribution to I_{11} only for $\bar{\kappa} > 0$.

Using (A-14) we have the following equivalent form

$$I_{11} = \frac{i}{2}e^{-\bar{\kappa}d}\int_{\tilde{C}} dw\, e^{-\frac{i\bar{\kappa}h}{\pi}\left(w+e^{w-1}\right)} \qquad (4\text{-}9)$$

where the path of integration in the w-plane is illustrated in Fig 3. Introduce the change of variable

$$\zeta = \frac{i\bar{\kappa}h}{\pi}e^{w-1} \qquad (4\text{-}10)$$

$(\bar{\kappa} > 0)$, then (3-8) is transformed into Hankel's integral representation of the Γ-function (Whittaker and Watson 1935, page 244) and we find

$$I_{11}(\bar{\kappa}) = \frac{\pi H(\bar{\kappa})e^{-|\bar{\kappa}|(d-h/2)}}{\Gamma\left(1 + i\frac{\bar{\kappa}h}{\pi}\right)}\left(\frac{|\bar{\kappa}|h}{e\pi}\right)^{\frac{i\bar{\kappa}h}{\pi}} \quad . \qquad (4\text{-}11)$$

Similarly it is readily deduced that

$$\bar{I}_{12}(\bar{\kappa}) = \frac{\pi H(-\bar{\kappa}) e^{-|\bar{\kappa}|(d-h/2)}}{\Gamma\left(1 - i\frac{\bar{\kappa}h}{\pi}\right)} \left(\frac{|\bar{\kappa}|h}{e\pi}\right)^{-i\frac{\bar{\kappa}h}{\pi}} \tag{4-12}$$

and therefore that

$$I_1(\bar{\kappa}) = I_{11}(\bar{\kappa}) + I_{12}(\bar{\kappa})$$

$$= \frac{\pi e^{-|\bar{\kappa}|(d-h/2)}}{\Gamma\left(1 + i\frac{\bar{\kappa}h}{\pi}\right)} \left(\frac{|\bar{\kappa}|h}{e\pi}\right)^{i\frac{\bar{\kappa}h}{\pi}} . \tag{4-13}$$

By means of an analogous procedure it may be shown that

$$I_2(\bar{\kappa}) = - I_1(\bar{\kappa}) . \tag{4-14}$$

Substituting these results into the expression (4-3) for the far field sound radiated to an observer located below the horizontal plane of flight of the aircraft, we obtain:

$$\frac{p(\underset{\sim}{r},t)}{\rho_0} = \frac{U_s v}{4\pi}\left(\frac{h}{r}\right)\left(\frac{\Omega\Lambda}{c}\right) \frac{\sin\bar{\theta}}{(1 - M\cos\theta)^2} \left(\frac{|\Omega|h\sqrt{1-M^2}}{\pi e U_s}\right)^{i\frac{\Omega h\sqrt{1-M^2}}{\pi U_s}} \times$$

$$\times \left\{ \frac{\cos\left[\frac{\Omega\ell \sin\bar{\theta}}{c(1-M^2)}\right]}{\sin\left[\frac{\Omega\ell\sin\bar{\theta}}{c(1-M^2)} - \Delta(e)\right]} + i\cos\Theta \right\} \times$$

$$\times \frac{\exp\left[-i\Omega(t - r/c) - \frac{|\Omega|}{U_s}(d - h/2)\sqrt{1-M^2}\right]}{\Gamma\left(1 + i\frac{\Omega h\sqrt{1-M^2}}{\pi U_s}\right)} \tag{4-15}$$

provided that $d > h$. Note that as the hydrodynamic length scale U_s/Ω of the harmonic eddy becomes small compared with the width h of the slot

$$\Gamma\left(1 + i\frac{\Omega h\sqrt{1-M^2}}{\pi U_s}\right) \sim \left\{\frac{|\Omega|h}{U_s}(1-M^2)^{\frac{1}{2}}\right\}^{\frac{1}{2}} e^{-\frac{|\Omega|h\sqrt{1-M^2}}{2U_s}}$$

and the acoustic response predicted by (4-15) decays exponentially with distance $d - h > 0$ of closest approach of the eddy to the leading edge of the slot. Also, provided that Ω is not close to one of the resonant frequencies $\Omega(\bar{\theta})$ of the slot, or that $\Omega\ell/c$ is small, the 'monopole' and 'dipole' contributions to the radiation field are of the same order of magnitude.

Case II: $0 < d < h$, eddy passing through the slot.

In this case the eddy interacts with both mouths A and B of the slot, and there are corresponding separate contributions to the radiation field provided respectively by the Green's function representations (A-36) and (A-39) of the Appendix.

It follows as before that for an observer at $\underset{\sim}{r}$ below the wing/flap system:

$$\frac{p(\underset{\sim}{r},t)}{\rho_0} = \frac{U_s v}{4\pi^2}\left(\frac{h}{r}\right)\left(\frac{\Omega\Lambda}{c}\right)\frac{\sin\bar{\theta}}{(1 - M\cos\theta)^2}\, e^{-i\Omega(t-r/c)} \times$$

$$\times \left\{ \frac{I_1(\bar{\kappa})\cos\left[\frac{\Omega\ell\sin\bar{\theta}}{c(1-M^2)}\right] - I_3(\bar{\kappa})e^{iM\Omega\ell/c(1-M^2)}}{\sin\left[\frac{\Omega\ell\sin\bar{\theta}}{c(1-M^2)} - \Delta(\Omega)\right]} - iI_2(\bar{\kappa})\cos\Theta \right\} \qquad (4\text{-}16)$$

where $I_j(\bar{\kappa})$ are defined as in (4-4), with $\phi_3^*(\underset{\sim}{Y})$ given implicitly by equation (A-18) of the Appendix. The path of integration in (4-4) is the contour $\mathrm{Im}\, z = d$ passing through the slot, *ie* above the branch cut $(-\infty + ih, ih)$ of the w-functions which defines the flap. We now find that

$$I_1(\bar{\kappa}) \equiv -I_2(\bar{\kappa})$$

$$= -i\Gamma\left(\frac{-i\bar{\kappa}h}{\pi}\right)\left(\frac{\bar{\kappa}h}{e\pi}\right)^{\frac{i\bar{\kappa}h}{\pi}} e^{-\frac{\bar{\kappa}h}{2}} \sinh(\bar{\kappa}d) \qquad (4\text{-}17)$$

and also that

$$I_3(\bar{\kappa}) = -i\Gamma\left(\frac{i\bar{\kappa}h}{\pi}\right)\left(\frac{\bar{\kappa}h}{e\pi}\right)^{-\frac{i\bar{\kappa}h}{\pi}} e^{-\bar{\kappa}\frac{h}{2}} \sinh(\bar{\kappa}[h-d]) \quad . \qquad (4\text{-}18)$$

Case III: $d < 0$, eddy passing above wing and flap.

The sound is produced by the interaction specified by the form (A-39) of the Green's function, *ie*, by diffraction radiation from the trailing edge B of the wing. The field at a point $\underset{\sim}{r}$ below the plane of flight of the aircraft becomes

$$\frac{p(\underset{\sim}{r},t)}{\rho_0} = -\frac{U_s v}{4\pi^2}\left(\frac{h}{r}\right)\left(\frac{\Omega\Lambda}{c}\right)\frac{\sin\bar{\theta}}{(1-M\cos\theta)^2} e^{-i\Omega(t-r/c)} \times$$

$$\times \frac{I_3(\bar{\kappa}) e^{iM\Omega\ell/c(1-M^2)}}{\sin\left[\frac{\Omega\ell\sin\bar{\theta}}{c(1-M^2)} - \Delta(\Omega)\right]} \quad . \qquad (4\text{-}19)$$

In the flyover plane ($\bar{\theta} = 90^\circ$) this represents monopole radiation corresponding to the reciprocating flow induced in the mouth A of the slot by the passage of the eddy. The contour integral $I_3(\bar{\kappa})$ may be evaluated in the manner described above, and in this case we obtain

$$\frac{p(\underset{\sim}{r},t)}{\rho_0} = -\frac{U_s v}{4\pi}\left(\frac{h}{r}\right)\left(\frac{\Omega\Lambda}{c}\right)\left(\frac{|\Omega|h\sqrt{1-M^2}}{e\pi U_s}\right)^{-\frac{i\Omega h\sqrt{1-M^2}}{\pi U_s}} \times$$

$$\times \frac{\sin\bar{\theta}\,\exp\left[-i\Omega(t-r/c) + \frac{|\Omega|}{U_s}(d-h/2)\sqrt{1-M^2} + \frac{iM\Omega\ell}{c(1-M^2)}\right]}{(1-M\cos\theta)^2\,\Gamma\left(1-\frac{i\Omega h\sqrt{1-M^2}}{\pi U_s}\right)\sin\left\{\frac{\Omega\ell\sin\bar{\theta}}{c(1-M^2)} - \Delta(\Omega)\right\}} \quad . \qquad (4\text{-}20)$$

5 DISCUSSION

In this section the theoretical results of sections 3 and 4 are examined in relation to:

(i) the Doppler amplification of the aerodynamic sound by forward flight of the aircraft;

(ii) the velocity dependence of the aerodynamic sound;

(iii) the sound radiated in the sideline direction.

To facilitate the discussion, introduce the definition

$$\ell_s = \frac{U_s}{\Omega} \tag{5-1}$$

of the eddy length scale associated with radian frequency Ω (relative to the aerofoil), and set $M_s = U_s/c$. We shall assume that ℓ_s is proportional to the effective width d of the turbulent boundary layer (*cf* equation (4-1)), so that in particular $\Omega d/U_s$ may be taken to be independent of the frequency.

(i) Doppler amplification

Confine attention to the flyover plane, for which $\phi = 0$, $\bar{\theta} = 90^o$. The result (4-15) for the sound generated by an eddy translating below the wing/flap configuration may then be expressed in the form:

$$\left(\frac{p}{\rho_0 c^2}\right)^2 \sim \frac{(M_s \ell/\ell_s)^6}{(1 - M\cos\theta)^4} \left| \frac{\cos\left(\frac{M_s \ell/\ell_s}{1 - M^2}\right)}{\sin\left(\frac{M_s \ell/\ell_s}{1 - M^2} - \Delta\right)} + \frac{i(\cos\theta - M)}{(1 - M\cos\theta)} \right|^2 \tag{5-2}$$

in which only those terms explicitly dependent on the eddy convection Mach number M_s and the flight velocity M have been retained. The definitions (A-21) and (A-30) of the Appendix may be used to show that Δ has the functional form:

$$\Delta = \frac{2\varepsilon}{\pi\sqrt{1 - M^2}} \left(\frac{M_s \ell}{\ell_s}\right) \left\{ \ell n \left[\frac{\varepsilon (M_s \ell/\ell_s)}{9.59\sqrt{1 - M^2}} \right] - \frac{\pi i}{2} \right\} \tag{5-3}$$

where

$$\varepsilon = \frac{h}{\ell} \ . \tag{5-4}$$

The ratio ℓ/ℓ_s of the slot length to the turbulence scale governs the efficiency with which a resonant response of the slot is excited. Since M_s

may be expected to be of the order of 0.3, resonant behaviour is more likely to occur for $\ell_s \ll \ell$.

We have seen in the previous section that the first term in the modulus-bars of (5-2) corresponds to a monopole source of sound associated with a reciprocating flow produced by the eddy in the mouth A of the slot. Indeed, the field shape of this component possesses the characteristic monopole, fourth power dependence on the Doppler factor $(1 - M \cos \theta)^{-1}$. The second component of the radiation is proportional to $(\cos \theta - M)/(1 - M \cos \theta)$, and by itself would experience an amplification of six Doppler factors on the sound pressure level. This source consists of a dipole whose axis is aligned parallel to the slot together with an omnidirectional quadrupole. The intensities of the dipole and quadrupole sources depend respectively on the sixth and eighth powers of the flow velocity, in agreement with the notions of the classical theory of aerodynamic sound (Ffowcs Williams, 1969). It is interesting to note that the 6-Doppler factor amplification of the dipole is in accord with the results of recent aerodynamic model problems investigated by Crighton (1975), Howe (1975) and Ffowcs Williams and Lovely (1976), whereas the field generated by an ideal (point) dipole is actually amplified in flight by only four Doppler factors. The difference arises because the dipole field of (5-2) may be ascribed to a distribution of sources in the aerofoil whose total strength must integrate to zero; the strength of the radiated sound thus depends on retarded time differences between these sources and this produces a single additional Doppler factor on the linear acoustic field.

It is clear from (5-2) that the effect of flight on the sound pressure level depends on the relative magnitudes of the monopole and the dipole-quadrupole sources, and this in turn is determined by the value of $M_s \ell / \ell_s$. Four Doppler factors would be expected at the lower frequencies for which the monopole field is dominant. In general, however, the variation cannot strictly be defined by a simple power of $(1 - M \cos \theta)^{-1}$.

When the turbulence interaction with the slot takes place on the upper surface of the wing, the result analogous to (5-2) is furnished by the purely monopole field of equation (4-20), and

$$\left(\frac{p}{\rho_0 c^2}\right)^2 \sim \frac{(M_s \ell/\ell_s)^6}{(1 - M \cos \theta)^4 \left| \sin\left(\frac{M_s \ell/\ell_s}{1 - M^2} - \Delta\right) \right|^2} \qquad (5\text{-}5)$$

for observer positions in the flyover plane, Δ being given by (5-3). In this case forward flight of the aircraft produces a conventional fourth-power Doppler amplification of the monopole source.

An analogous, but more complicated expression may also be written down for the case in which the eddy convects through the slot.

(ii) Velocity dependence of the aerodynamic sound

The results (5-2) and (5-5) indicate that as the convection Mach number $M_s \to 0$ the radiation is dominated by a monopole field whose intensity varies as M_s^4. For larger values of $M_s \ell/\ell_s$ the behaviour is more complicated. In order to examine the general situation write

$$\overline{p^2} = c \cdot \left(\frac{M_s \ell}{\ell_s}\right)^n \qquad (5\text{-}6)$$

where c is a constant, and $n \equiv n\,(M_s \ell/\ell_s, \theta)$ is an effective velocity index. This index can be calculated from equations (5-2) and (5-5).

Fig 4 exhibits the variation of the velocity index for the sound generated by above-the-wing-turbulence (equation (5-5)) for $M = 0.2$. For $M_s \ell/\ell_s$ less than about unity, n is approximately constant, equal to 4.6 for $\varepsilon = 0.1$, increasing through 5.1 at $\varepsilon = 0.3$ to $n = 5.4$ at $\varepsilon = 0.5$. The fourth power asymptotic limit is attained only for $M_s \ell/\ell_s$ much less than 0.1. Large fluctuations in n occur at the smaller values of ε and are produced by the resonances of the slot. Increasing ε modifies the resonant frequencies and also increases the radiation damping of the oscillations in the slot. Other dissipative mechanisms have not been considered here, but it is likely that losses in the boundary layers of the slot are particularly important near the resonance frequencies, and in practice, therefore, the velocity index curve may be expected to conform principally with the pictures presented in Fig 4 for $\varepsilon = 0.3$ or 0.5.

In Fig 5 the effective velocity index n has been plotted against $M_s \ell/\ell_s$ for the case given by (5-2) of an eddy passing below the wing. We have taken $M = 0.2$ and $\varepsilon = 0.5$ as being the most representative values in practice (smaller values of ε produce a rather more sharply peaked variation in n), and present the results for three directions $\theta = 45^\circ$, 90°, 135°. A fourth power law prevails only for $M_s \ell/\ell_s$ very much smaller than 0.1. For $0.1 < M_s \ell/\ell_s < 1$ the velocity index $n \simeq 5.4$. The large variations at $\theta = 90^\circ$ occur because

this is the null direction of the dipole component of the radiation and changes in the value of $\cos\{(M_s\ell/\ell_s)/(1 - M^2)\}$ in (5-2) are more significant than at other angles.

(iii) The sideline noise

We shall now use equation (4-20) for the sound generated by a disturbance convecting along the upper surface of the aerofoil to illustrate the principal features of the sound radiated to the side of the flight path.

Consider the case $\theta = 90^o$. The sideline direction is specified by the azimuthal angle ϕ , $\phi = 0$ being the flyover plane. From the Table in the Appendix it transpires that $\sin\bar{\theta} = \cos\phi + 0(M^2)$. It follows from (4-20) that the sideline variation in the field shape corresponds to that of a vertically orientated dipole except at the lower frequencies, or when $(\Omega\ell/c)\sin\bar{\theta}$ becomes small, where the variation is more like that of a monopole (*cf* section 3, above). It is perhaps significant that monopole patterns of sideline variation have actually been observed by Fethney (1975) in experiments involving four different aircraft, although the results he presents are all for aircraft in the 'clean' configuration with flaps retracted.

Reference to equation (4-20) indicates that the acoustic response is maximal near the frequency

$$\Omega = \frac{\pi c(1 - M^2)}{\ell \sin\bar{\theta}} \qquad (5\text{-}7)$$

which increases as the observer moves into the sideline direction. Such variations in the peak frequencies of airframe noise have been reported in the literature (see, *eg*, Hardin 1976), and it is of interest to examine in detail the spectral variations to be expected in the present case.

Set

$$\Omega_p = \frac{\pi c(1 - M^2)}{\ell} \quad , \qquad (5\text{-}8)$$

the peak frequency in the flyover plane, and define a dimensionless frequency f by

$$f = \frac{\Omega}{\Omega_p} \quad . \qquad (5\text{-}9)$$

Then we have from (4-20)

$$\Phi(f,\phi) \equiv \overline{\left(\frac{p}{\rho_0 c^2}\right)^2}$$

$$= \frac{\overline{Sv^2} f \sin^2\bar{\theta}\left\{1 - \exp\left(-\frac{2\pi\varepsilon f(1 - M^2)^{3/2}}{M_s}\right)\right\}}{\left|\sin\left(\pi f \sin\bar{\theta} - \Delta(f)\right)\right|^2} \qquad (5\text{-}10)$$

where S depends on M, M_s and the observer distance r, which we shall assume to be fixed. Also

$$\Delta(f) = 2\varepsilon f \sin\bar{\theta}\sqrt{1 - M^2}\left\{\ell n\left[\frac{\varepsilon f \sin\bar{\theta}\sqrt{1 - M^2}}{3.05}\right] - \frac{\pi i}{2}\right\} \qquad (5\text{-}11)$$

and the overbar in (5-10) denotes an ensemble average.

Equation (5-10) defines the acoustic spectrum in terms of the turbulence spectrum function $\overline{v(f)^2}$ (*cf* definition (4-1)). For simplicity take the case of 'white noise' excitation ($\overline{v^2}$ = constant). Fig 6 depicts the variation in the shape and level of the corresponding acoustic spectrum (expressed in dB relative to $\Phi(f = 1, \phi = 0)$ at $\phi = 0^\circ, 30^\circ, 60^\circ$, for $M_s = 0.8\ M$, $M = 0.2$ and $\varepsilon = h/\ell = 0.1$. With increasing values of the sideline angle ϕ the spectral peaks are displaced to higher frequencies; the absolute levels are reduced at the higher frequencies (corresponding to a dipole-like directivity). Monopolar behaviour obtains for $f \lesssim 0.5$ for which there is little or no change in the spectral levels in the sideline direction.

The Kutta condition

In obtaining the theoretical results discussed in this Report no mention has been made of the nature of the perturbed flow in the vicinity of the trailing edge B of the wing. This will possess a singularity at the edge unless allowance is made for the shedding of additional vorticity, *ie*, unless a Kutta condition is imposed. On a strictly linear theory, in which the incident turbulence and the shed vorticity convect at a common velocity U_s, it may be shown that the sound produced by the eddy during the interaction with the edge B is exactly cancelled by that generated by the shed vorticity (*cf* Howe 1976, 1977).

In particular for an eddy passing through the slot, sound is produced solely through the interaction with the *leading* edge A when the Kutta condition is applied.

In practice, however, the convection velocities of the incident eddy and the shed vorticity are not the same, but are characteristic of the prevailing local boundary layer conditions. Complete cancellation of the radiated sound field is no longer possible, and the essential features of the radiation will be in accord with the results derived in the previous section and discussed above, (*cf* the analogous results obtained by Howe (1977) for a trailing edge).

The effect of finite flap chord

Our analysis has been based on the assumption that the chord of the flap is large compared with the acoustic wavelength. It is of interest to discuss the qualitative changes in the sound field which are expected to occur as the wavelength increases relative to the chord. This will be particularly relevant at the lower frequencies, below that of the first resonance frequency of the slot, for which the acoustic field corresponds approximately to that generated by a monopole source.

The monopole radiation from the slot is characterized by an omnidirectional field shape whose intensity varies approximately as the fourth power of the turbulence Mach number. As the wavelength increases, and becomes comparable with the chord, the sound generated by this monopole source exhibits directional characteristics arising from the interference between the direct radiation and that arriving after diffraction at the trailing edge of the flap. The envelope intensity of the radiation would still vary approximately as M_s^4 .

When the wavelength exceeds the chord of the flap there is a progressive tendency for the unsteady flow induced about the trailing edge of the flap to provide a hydrodynamic short circuit of the monopole flow through the slot. This eventually reduces the efficiency with which sound is generated to that characteristic of turbulence located near a half-plane (the wing). The field is now strongly directional, peaking in the forward arc ($\theta < 90^\circ$) and the sound pressure level varies as the fifth power of the turbulence Mach number. (Ffowcs Williams and Hall (1970)).

6 CONCLUSION

The principal results of the analysis of the slot noise mechanism by the simplified mechanism described in this Report may be summarized as follows:

(1) Above-the-wing-turbulence generates a monopole field in the flyover plane which is amplified by four powers of the Doppler factor $(1 - M \cos \theta)^{-1}$ in forward flight. There is no simple dependence on the Doppler factor when the turbulence convects below the wing and/or through the slot, except at very low frequencies when the simple monopole field is recovered.

(2) For acoustic frequencies less than about half that of the lowest resonant frequency of the slot the radiation is essentially that of a monopole source whose intensity varies roughly as the fourth or fifth power of the velocity. At higher frequencies the velocity dependence fluctuates because of resonances. When account is taken of the action of viscous dissipation within the slot it appears that in practice the sound pressure level will be proportional to U_s^n where n lies between 4 and 6.

(3) Sideline noise exhibits dipole characteristics (dipole axis in the vertical direction) except at frequencies less than about half the lowest resonance frequency of the slot, or at high sideline angles, greater than about 70°, say, in which case the variation is more like that of a monopole. The spectral peaks of the acoustic field are reduced and shifted to higher frequencies as the sideline angle increases.

The author gratefully acknowledges the benefit he has derived from discussions of the material of this Report with E.G. Broadbent, FRS.

Appendix

THE GREEN'S FUNCTION FOR A TWO-DIMENSIONAL SLOT

The advanced potential solution $G(\underset{\sim}{x},\underset{\sim}{y},t,\tau)$ of equation (2-5) must be a function of $t - \tau$, and therefore $\partial G/\partial\tau \equiv \partial G/\partial t$ and the calculation of G is equivalent to the determination of the retarded solution of the reverse flow equation:

$$\left\{\frac{1}{c^2}\left(\frac{\partial}{\partial t} + U\frac{\partial}{\partial y_1}\right)^2 - \frac{\partial^2}{\partial y_j^2}\right\} G = \delta(\underset{\sim}{x} - \underset{\sim}{y})\delta(t - \tau) \quad . \tag{A-1}$$

This equation defines a reciprocal problem in which the source on the right-hand-side is triggered at time τ at the observer position $\underset{\sim}{x}$. It is required to determine the behaviour of G at points $\underset{\sim}{y}$ close to the slot in the case in which $\underset{\sim}{x}$ is many characteristic wavelengths from the slot. Introduce the Prandtl-Glauert transformation

$$\left.\begin{aligned} \underset{\sim}{X} \equiv (X_1,X_2) &= \left(\frac{x_1}{\sqrt{1 - M^2}}, x_2\right) \\ \underset{\sim}{Y} \equiv (Y_1,Y_2) &= \left(\frac{y_1}{\sqrt{1 - M^2}}, y_2\right) \end{aligned}\right\} \tag{A-2}$$

and define $\phi(\omega,k_3) \equiv \phi(\underset{\sim}{X},\underset{\sim}{Y},\omega,k_3)$ by means of

$$G(\underset{\sim}{x},\underset{\sim}{y},t,\tau) = \frac{1}{(2\pi)^2\sqrt{1 - M^2}} \int\int_{-\infty}^{\infty} \phi(\omega,k_3) e^{i\{k_3(x_3-y_3)-MK(Y_1-X_1)-\omega(t-\tau)\}} d\omega dk_3 \quad , \tag{A-3}$$

where

$$K = \frac{\omega/c}{\sqrt{1 - M^2}} \quad . \tag{A-4}$$

The potential function ϕ satisfies

$$\frac{\partial^2\phi}{\partial Y_1^2} + \frac{\partial^2\phi}{\partial Y_2^2} + \gamma^2\phi = -\delta(\underset{\sim}{X} - \underset{\sim}{Y}) \tag{A-5}$$

in which γ is given by

$$\gamma = \begin{cases} \text{sgn } (K) \\ + i \end{cases} \left| K^2 - k_3^2 \right|^{\frac{1}{2}} \qquad \text{(A-6)}$$

according as $K^2 \gtrless k_3^2$. The problem thus reduces to the determination of ϕ subject to $\partial\phi/\partial Y_2 = 0$ on the rigid surfaces of the 'wing' and 'flap'.

We shall assume that the observer location $\underset{\sim}{X}$ lies below the wing/flap system many wavelengths from the end A. Let $\bar{\underset{\sim}{X}}$ denote the image point of $\underset{\sim}{X}$ in either of the planes forming the slot (the difference in the values of $\bar{\underset{\sim}{X}}$ for each of the half-planes is negligible on a wavelength scale if the width of the slot is compact).

The two-dimensional source at $\underset{\sim}{X}$ on the right of equation (A-5) generates a cylindrical wave

$$\phi_i = \frac{i}{4} H_0^{(1)}(\gamma|\underset{\sim}{Y} - \underset{\sim}{X}|) \qquad \text{(A-7)}$$

which is incident on the slot from $X_2 > 0$. This induces a (two-dimensional) reciprocating flow in the mouth at A and the principal terms in the field ϕ_R say, scattered back from the slot therefore comprise monopole radiation from A together with the radiation from an image source at $\bar{\underset{\sim}{X}}$:

$$\phi_R = \frac{i}{4} H_0^{(1)}(\gamma|\underset{\sim}{Y} - \bar{\underset{\sim}{X}}|) + \alpha_1 H_0^{(1)}(\gamma|\underset{\sim}{Y}|) \quad . \qquad \text{(A-8)}$$

In this expression it is assumed that the origin of coordinates is located at the end A of the slot and that the reciprocal observer position $\underset{\sim}{Y}$ satisfies $|\underset{\sim}{Y}| >> h$, where h is the slot width.

In the immediate vicinity of the mouth A the flow has the characteristics of an ideal irrotational, incompressible flow and we may write

$$\phi = \phi_0 + \beta_1 \phi_1^*(\underset{\sim}{Y}) + \beta_2 \phi_2^*(\underset{\sim}{Y}) + \ldots \qquad \text{(A-9)}$$

where the terms shown explicitly represent the leading contribution to an asymptotic expansion in which $\gamma h << 1$ is the small parameter. The functions ϕ_0, β_1, β_2 depend on K and k_3. The space dependent terms $\phi_1^*(\underset{\sim}{Y})$, $\phi_2^*(\underset{\sim}{Y})$ are solutions of Laplace's equation which satisfy the condition of vanishing normal velocity on the surfaces of the slot. They have the following physical interpretation:

(i) $\beta_1\phi_1^*(\underset{\sim}{Y})$ describes the reciprocating flow in the mouth at A;

(ii) $\beta_2\phi_2^*(\underset{\sim}{Y})$ accounts for a local, source-induced 'streaming' flow past A in a direction parallel to the slot, but which does not involve a net flux of fluid through the slot (see below).

Above the slot (*ie* in $Y_2 < 0$), the field consists entirely of monopole radiation from the mouth B, and if $\underset{\sim}{Y} = -\underset{\sim}{L}$ is the vector position of the edge at B (*ie* $\underset{\sim}{L} \equiv (L,0) = (\ell/\sqrt{1 - M^2}\ , 0)$), we have for $|\underset{\sim}{Y} + \underset{\sim}{L}| >> h$

$$\phi = \alpha_2 H_0^{(1)}(\gamma|\underset{\sim}{Y} + \underset{\sim}{L}|) \quad . \tag{A-10}$$

The local reciprocating flow at B has a form analogous to (A-9) except that there is no source-induced streaming past the mouth in the ambient medium:

$$\phi = \phi_1 + \beta_3\phi_3^*(\underset{\sim}{Y}) + \ldots \quad . \tag{A-11}$$

Finally, inside the slot and at distances exceeding h from either end, the motion is one-dimensional and has the simple representation

$$\phi = Ae^{i\gamma Y_1} + Be^{-i\gamma Y_1} \tag{A-12}$$

Specification of the potential functions

The functions $\phi_j^*(\underset{\sim}{Y})$ may be determined in the usual way from analytic function theory.

Set

$$z = Y_1 + iY_2 \tag{A-13}$$

with the origin of coordinates at the point 0 of Fig 1b.

First $\phi_1^*(\underset{\sim}{Y})$ may be defined as the real part of $w_1(z)$ where

$$z = \frac{h}{\pi}\left[w_1 + e^{w_1 - 1}\right] \quad . \tag{A-14}$$

This implicit relation describes irrotational flow out of the mouth A when the slot length $\ell >> h$ (Lamb, 1932 page 73). If $w_1 = \phi_1^* + i\psi_1^*$, the streamlines $\psi_1^* = 0\ ,\ \pi$ define respectively the wing and flap. We shall require the

asymptotic forms of $\phi_1^*(\underset{\sim}{Y})$ as $|\underset{\sim}{Y}| \to \infty$ below the wing (*ie* in $Y_2 > 0$) and also within the slot. It follows readily from (A-14) that

$$\left.\begin{aligned} \phi_1^*(\underset{\sim}{Y}) &\sim \ell n\left(\frac{\pi e}{h}\,|\underset{\sim}{Y}|\right) && \text{outside the slot,} \\ &\sim \pi Y_1/h && \text{inside the slot.} \end{aligned}\right\} \tag{A-15}$$

Similarly $\phi_2^*(\underset{\sim}{Y})$ is the real part of w_2 where

$$z = \frac{h}{\pi}\left[w_2 + \ell n(ew_2)\right] , \tag{A-16}$$

from which it follows that

$$\left.\begin{aligned} \phi_2^*(\underset{\sim}{Y}) &\sim \pi Y_1/h && \text{outside the slot,} \\ &\sim 0 && \text{in the slot.} \end{aligned}\right\} \tag{A-17}$$

Finally the function $\phi_3^*(\underset{\sim}{Y})$ can be deduced from $\phi_1^*(\underset{\sim}{Y})$ by replacing z by $ih - L - z$, *ie*,

$$z = ih - L - \frac{h}{\pi}\left[w_3 + e^{w_3^{-1}}\right] , \tag{A-18}$$

and

$$\left.\begin{aligned} \phi_3^*(\underset{\sim}{Y}) &\sim \ell n\left(\frac{\pi e|\underset{\sim}{Y} + \underset{\sim}{L}|}{h}\right) && \text{above the wing,} \\ &\sim -\frac{\pi}{h}\,(Y_1 + L) && \text{in the slot.} \end{aligned}\right\} \tag{A-19}$$

We shall see below that for the applications considered in this paper it is necessary to determine only the values of the coefficients $\beta_j (j = 1,2,3)$ of the potential functions $\phi_j^*(\underset{\sim}{Y})$. This can be done by equating the various alternative expressions for ϕ written down above in regions of common validity (*cf* Rayleigh, 1945, page 198).

First from (A-7) and (A-8) the field below the wing at points $\underset{\sim}{Y}$ located much less than a characteristic wavelength from A yet at the same time satisfying $|\underset{\sim}{Y}| >> h$, may be set in the form

$$\begin{aligned}\phi &= \phi_i + \phi_R \\ &\simeq 2Z\left[1 - i\gamma Y_1 \cos\Theta\right] \\ &\quad + \alpha_1\left[\chi + \frac{2i}{\pi}\,\ell n\,(\gamma|\underset{\sim}{Y}|)\right]\end{aligned} \tag{A-20}$$

where

$$\left.\begin{aligned} Z &= \frac{1}{4}\sqrt{\frac{2i}{\pi\gamma|\underset{\sim}{X}|}}\, e^{i\gamma|\underset{\sim}{X}|}\,, \\ \chi &= \frac{2i}{\pi}\,(C - \ell n\ 2)\,, \\ C &= 0.57722 \qquad \text{(Euler's constant)}, \\ \cos\Theta &= X_1/|\underset{\sim}{X}|\ . \end{aligned}\right\} \tag{A-21}$$

The corresponding asymptotic form of (A-9) yields the following approximate representation

$$\phi = \phi_0 + \beta_1\,\ell n\left(\frac{\pi e|\underset{\sim}{Y}|}{h}\right) + \beta_2\,\frac{\pi Y_1}{h} + \ldots \tag{A-22}$$

use having been made of (A-15) and (A-17). Equating coefficients in (A-20) and (A-22), we obtain:

$$\left.\begin{aligned} \phi_0 + \beta_1\,\ell n\left(\frac{\pi e}{h}\right) &= 2Z + \alpha_1\left(\chi + \frac{2i}{\pi}\,\ell n\ \gamma\right) \\ \beta_1 &= \frac{2i}{\pi}\,\alpha_1 \\ \pi\beta_2/h &= -\,2i\gamma Z\cos\Theta\ . \end{aligned}\right\} \tag{A-23}$$

Similarly at points Y_1 within the slot such that $|Y_1| >> h$ but $|\gamma Y_1| << 1$ we have from (A-15) and (A-17)

$$\phi \sim \phi_0 + \pi\,\frac{\beta_1 Y_1}{h} \tag{A-24}$$

which must match with the corresponding expansion derived from the internal wave representation (A-12), viz:

$$\phi \sim A + B + i\gamma Y_1 (A - B) \quad . \tag{A-25}$$

Thus

$$\left.\begin{aligned} \phi_0 &= A + B \\ \frac{\pi\beta_1}{h} &= i\gamma(A - B) \quad . \end{aligned}\right\} \tag{A-26}$$

Conditions analogous to (A-23) and (A-26) may be written down for the end B of the slot. These are:

$$\left.\begin{aligned} \phi_1 + \beta_3 \ln\left(\frac{\pi e}{h}\right) &= \alpha_2\left(\chi + \frac{2i}{\pi} \ln \gamma\right) \\ \beta_3 &= \frac{2i\alpha_2}{\pi} \end{aligned}\right\} \tag{A-27}$$

and

$$\left.\begin{aligned} \phi_1 &= Ae^{-i\gamma L} + Be^{i\gamma L} \\ \frac{\pi\beta_3}{h} &= -i\gamma\left[Ae^{-i\gamma L} - Be^{i\gamma L}\right] \quad . \end{aligned}\right\} \tag{A-28}$$

The system of equations ((A-23), (A-26), (A-27), (A-28)), may now be used to express the coefficients β_j in terms of Z, the incident wavefield. Performing the elementary reductions we obtain:

$$\left.\begin{aligned} \beta_1 &= \frac{2\gamma h Z \cos \gamma L}{\pi \sin(\gamma L - \Delta)} \\ \beta_2 &= -\frac{2i\gamma h Z}{\pi} \cos \Theta \\ \beta_3 &= -\frac{2\gamma h Z}{\pi \sin(\gamma L - \Delta)} \end{aligned}\right\} \tag{A-29}$$

where

$$\Delta = \frac{2\gamma h}{\pi}\left\{\ln\left(\frac{\gamma h}{\pi e}\right) - \frac{\pi i \chi}{2}\right\} \quad . \tag{A-30}$$

These coefficients determine the response of the fluid in the vicinity of the ends A and B of the slot due to the source at $\underset{\sim}{X}$. Observe that Δ is a

complex number whose imaginary part fixes the peak values attained by β_1 , β_3 when $\gamma L \simeq n\pi$ (n integral), *ie*, for frequencies close to the natural (organ pipe) modes of the slot. This resonant response is associated with the reciprocating flows into the mouths A and B of the slot described respectively by the local components $\beta_1\phi_1^*(\underset{\sim}{Y})$ and $\beta_3\phi_3^*(\underset{\sim}{Y})$ of the potential ϕ . On the contrary β_2 exhibits no such resonant behaviour because the streaming flow $\beta_2\phi_2^*(\underset{\sim}{Y})$ does not penetrate beyond a distance $\sim O(h)$ into the mouth at A.

Note that in general $|\Delta| << |\gamma L|$ since h/ℓ is small. The imaginary part of Δ takes account of radiation damping whereby resonant oscillations in the slot decay through the emission of sound waves into free space from the mouths A and B. The real part of Δ gives the so-called Helmholtz 'end-correction'.

Next consider the local representation (A-9) of the flow induced near the mouth A by the source at $\underset{\sim}{X}$. It follows from equation (A-3) that for points $\underset{\sim}{Y}$ in the vicinity of A

$$G(\underset{\sim}{x},\underset{\sim}{y},t,\tau) = \frac{1}{(2\pi)^2\sqrt{1-M^2}} \iint_{-\infty}^{\infty} \left\{ \phi_0 + \beta_1\phi_1^*(\underset{\sim}{Y}) + \beta_2\phi_2^*(\underset{\sim}{Y}) + \ldots \right\} \times$$

$$\times \exp\left[i\left(k_3(x_3 - y_3) - MK(Y_1 - X_1) - \omega(t - \tau) \right) \right] d\omega dk_3 \ . \quad \text{(A-31)}$$

When this expression for the Green's function is used in the convolution integral (3-1), which determines the aerodynamic sound generated by the transverse component ω_3 of the vorticity, it is apparent that there will be no contribution from the term in ϕ_0 since it does not involve $\underset{\sim}{Y}$. Also, in deriving (3-1) the contribution to the radiation furnished by the ω_2-component of vorticity has been neglected. To justify this, note first of all that it would involve a convolution product of the form

$$\int \omega_2(y_1 + U_s\tau, y_2, y_3) \frac{\partial G}{\partial y_3}(\underset{\sim}{x},\underset{\sim}{y},t,\tau) d^3\underset{\sim}{y} d\tau \ .$$

In evaluating this integral the term in ϕ_0 in (A-31) gives an acoustic field of frequency $\omega = 0$ and vanishes identically; the contribution from the terms in β_j (j = 1,2) are

$$O\left(k_3/(\partial\phi_j^*/\partial y_2) \right) \sim O(k_3 h) << 1$$

relative to the corresponding radiation from the transverse (or ω_3) component of vorticity, and may therefore be neglected. These conclusions are an immediate consequence of the fact that, for an observer located in the far field, the integration with respect to k_3 in (A-31) may be performed by the method of stationary phase from which it follows that the integral is determined principally by those values of k_3 near

$$k_3 = K \cos \bar{\theta} \equiv \frac{(\omega/c) \cos \bar{\theta}}{\sqrt{1 - M^2}} ,$$

where

$$\left.\begin{aligned} \cos \bar{\theta} &= (x_3 - y_3)/R \\ R &= \sqrt{X_1^2 + X_2^2 + (x_3 - y_3)^2} \end{aligned}\right\} . \qquad \text{(A-32)}$$

The explicit form of the relevant portion of the Green's function $G(\underset{\sim}{x},\underset{\sim}{y},t,\tau)$ may be deduced from (A-31) by discarding ϕ_0, substituting for β_1, β_2 from (A-29) and for Z from (A-21):

$$G(\underset{\sim}{x},\underset{\sim}{y},t,\tau) = \frac{h}{(2\pi)^3\sqrt{1 - M^2}} \sqrt{\frac{2i}{\pi|\underset{\sim}{X}|}} \iint_{-\infty}^{\infty} \sqrt{\gamma} \left\{ \frac{\phi_1^*(\underset{\sim}{Y}) \cos \gamma L}{\sin (\gamma L - \Delta)} - i\phi_2^*(\underset{\sim}{Y}) \cos \Theta \right\} e^{i\left[k_3(x_3-y_3)+\gamma|\underset{\sim}{X}|-MK(Y_1-X_1)-\omega(t-\tau)\right]} dk_3 d\omega . \qquad \text{(A-33)}$$

Introduce the change of variable

$$k_3 = K \cos \psi$$

and, for large $(|\underset{\sim}{X}|, x_3 - y_3)$, perform the ψ-integration by stationary phase to obtain:

$$G(\underset{\sim}{x},\underset{\sim}{y},t,\tau) = \frac{2h \sin \bar{\theta}}{(2\pi)^3 Rc(1 - M^2)} \int_{-\infty}^{\infty} \omega \left\{ \frac{\phi_1^*(\underset{\sim}{Y}) \cos\left(\frac{\omega \ell \sin \bar{\theta}}{c(1 - M^2)}\right)}{\sin\left(\frac{\omega \ell \sin \bar{\theta}}{c(1 - M^2)} - \Delta(\bar{\theta})\right)} - i\phi_2^*(\underset{\sim}{Y}) \cos \Theta \right\} e^{-i\omega\left[t-\tau-(R+MX_1)/c\sqrt{1-M^2}\right]} d\omega . \qquad \text{(A-34)}$$

In obtaining this result it has been noted that, for a source point $\underset{\sim}{Y}$ located well within an acoustic wavelength of the mouth A of the slot, the contribution MKY_1, in the exponent of (A-33) may be neglected. Also from (A-30), $\Delta(\bar{\theta})$ assumes the functional form

$$\Delta(\bar{\theta}) = \frac{2\omega h \sin\bar{\theta}}{\pi c\sqrt{1-M^2}} \left\{ \ell n \left[\frac{\left(\frac{\omega h}{c}\right)\sin\bar{\theta}}{\pi e\sqrt{1-M^2}} \right] - \frac{\pi i}{2}\chi \right\} . \qquad \text{(A-35)}$$

It remains to express $G(\underset{\sim}{x},\underset{\sim}{y},t,\tau)$ in terms of the retarded coordinates (r,θ,ϕ) defined by (2-10) and which give the location of the observer at $\underset{\sim}{x}$ relative to the aircraft at the time of emission of the sound. To do this we make use of the transformation formulae listed in the Table to obtain:

$$G(\underset{\sim}{r},\underset{\sim}{y},t,\tau) = \frac{2h\sin\bar{\theta}}{(2\pi)^3 rc(1-M\cos\theta)\sqrt{1-M^2}} \int_{-\infty}^{\infty} \omega \left[\frac{\phi_1^*(\underset{\sim}{Y})\cos\left(\frac{\omega\ell\sin\bar{\theta}}{c(1-M^2)}\right)}{\sin\left(\frac{\omega\ell\sin\bar{\theta}}{c(1-M^2)} - \Delta(\bar{\theta})\right)} - i\phi_2^*(\underset{\sim}{Y})\cos\Theta \right] e^{-i\omega[t]}\, d\omega \qquad \text{(A-36)}$$

where

$$[t] = t - \tau - \frac{r}{c} . \qquad \text{(A-37)}$$

Equation (A-36) gives the approximate form of the Green's function when the source point $\underset{\sim}{y}$ is located well within an acoustic wavelength of the end A of the slot. For an observer located in the flyover plane ($\phi = 0$) it follows from the Table that $\sin\bar{\theta} = 1$. The first term in the square brackets of (A-36) may then be recognized as characterizing a monopole and the second a dipole-quadrupole combination (*cf* the discussion of section 5).

In the particular case in which the frequency ω of the aerodynamic source is sufficiently small that $\omega\ell/c \ll 1$, *ie*, in which the wavelength greatly exceeds the length of the slot, the first term in the square brackets of (A-36) is very much larger than the second. If, in addition, $h \ll \ell$, it follows that in a first approximation the ω-integration yields a δ-function and we have

$$G(\underset{\sim}{r},\underset{\sim}{y},t,\tau) = \frac{h\sqrt{1-M^2}}{2\pi^2\ell r(1-M\cos\theta)} \phi_1^*(\underset{\sim}{Y})\delta(t-\tau-r/c) . \qquad \text{(A-38)}$$

Table of coordinate transformations

Reference frame	
$\underset{\sim}{x}$ or $\underset{\sim}{X}$	(r, θ, ϕ)
x_1	$r(\cos\theta - M)$
x_2	$r \sin\theta \cos\phi$
$x_3 - y_3$	$r \sin\theta \sin\phi$
$R \equiv \sqrt{X_1^2 + X_2^2 + (x_3 - y_3)^2}$	$r(1 - M\cos\theta)/\sqrt{1 - M^2}$
$\lvert\underset{\sim}{X}\rvert \equiv \sqrt{X_1^2 + X_2^2}$	$r\left[(\cos\theta - M)^2 + (1 - M^2)\sin^2\theta\cos^2\phi\right]^{\frac{1}{2}}/\sqrt{1 - M^2}$
$\cos\Theta \equiv \dfrac{X_1}{\lvert\underset{\sim}{X}\rvert}$	$\dfrac{\cos\theta - M}{\left[(\cos\theta - M)^2 + (1 - M^2)\sin^2\theta\cos^2\phi\right]^{\frac{1}{2}}}$
$\sin\bar{\theta} \equiv \dfrac{\lvert\underset{\sim}{X}\rvert}{R}$	$\dfrac{\left[(\cos\theta - M)^2 + (1 - M^2)\sin^2\theta\cos^2\phi\right]^{\frac{1}{2}}}{(1 - M\cos\theta)}$
$\dfrac{R + MX_1}{\sqrt{1 - M^2}}$	r

Similarly, when the source point $\underset{\sim}{y}$ is located well within an acoustic wavelength of the mouth B of the slot, the appropriate form of the Green's function $G(\underset{\sim}{r},\underset{\sim}{y},t,\tau)$ may be deduced from (A-11), (A-29) to be

$$G(\underset{\sim}{r},\underset{\sim}{y},t,\tau) = \frac{-2h\sin\bar{\theta}}{(2\pi)^3 rc(1 - M\cos\theta)\sqrt{1 - M^2}} \int_{-\infty}^{\infty} \frac{\omega\phi_3^*(\underset{\sim}{Y})e^{-i\omega\left\{[t] - M\ell/c(1-M^2)\right\}}}{\sin\left[\dfrac{\omega\ell\sin\bar{\theta}}{c(1 - M^2)} - \Delta(\bar{\theta})\right]} d\omega \quad \ldots\ldots \text{(A-39)}$$

where, as before, the observer is located at $\underset{\sim}{r}$ below the wing/flap system. This result shows that the acoustic response below the aircraft to a disturbance at the 'upper' end B of the slot exhibits the properties of a monopole. Note that the essential difference between the monopole contributions of (A-36), (A-39) is the presence of the factor $\cos\left[\omega\ell \sin\bar{\theta}/c(1 - M^2)\right]$ in the former as compared with $\exp\left[i\omega M\ell/c(1 - M^2)\right]$ in the latter. This takes account of the additional time delay $\sim \ell(\sin\bar{\theta} + M)/c(1 - M^2)$ which must be allowed for a source located near B and radiating through the mouth A in the presence of the mean flow U in the direction AB.

Again, in the case of a compact slot $(\omega\ell/c << 1)$, (A-39) reduces to a form analogous to (A-38), viz:

$$G(\underset{\sim}{r},\underset{\sim}{y},t,\tau) = \frac{-h\sqrt{1 - M^2}}{2\pi^2\ell r(1 - M\cos\theta)}\,\phi_3^*(\underset{\sim}{Y})\,\delta\left(t - \tau - \frac{r}{c}\right) . \qquad (A\text{-}40)$$

The case of a short slot: $h \gtrsim \ell$

The analysis leading to the representations (A-36), (A-39) of the Green's function was based on the assumption that the local incompressible flows at A, B are independent in the sense that, in the reciprocal (or adjoint) problem determining G, the flow within the slot is uniform and parallel to the walls of the slot (*cf* Fig 2). This should be an adequate representation of the motion in the slot provided that h/ℓ is small, and this assumption is made in the applications of the main text. In practice, of course, the slot contracts substantially in the flow direction, and the effective mean value of h/ℓ may certainly be expected to be less than 0.25, say.

It is perhaps of interest to quote the form assumed by the Green's function when h/ℓ is not small. The derivation of $G(\underset{\sim}{r},\underset{\sim}{y},t,\tau)$ follows closely the procedure outlined above. The main difference is the absence of an interior wave field (A-12). In the reciprocal problem the flow in the neighbourhood of the slot is defined by a potential function of the form

$$\phi = \phi_2 + \beta_4\phi_4^*(\underset{\sim}{Y}) \qquad (A\text{-}41)$$

where ϕ_2, β_4 are functions of K, k_3. The appropriate form for $\phi_4^*(\underset{\sim}{Y})$ which describes potential flow through the slot, may be deduced from complex variable theory to be the real part of W_4 where

$$z + \frac{\ell}{2\sqrt{1 - M^2}} = \frac{h}{\pi}\left[W_4 + \mu \cosh W_4\right] . \qquad (A\text{-}42)$$

The value of the real constant μ determines the degree of overlap of the half-planes which represent the wing and flap *ie*, it determines the length ℓ of the slot. In fact it may be shown that

$$\frac{\ell}{h} = \frac{2\sqrt{1 - M^2}}{\pi}\left\{\sinh^{-1}\left(\frac{1}{\mu}\right) - \sqrt{1 + \mu^2}\right\} . \qquad (A\text{-}43)$$

There is no overlap ($\ell = 0$) for $\mu = 0.6628$; ℓ/h increases as $\mu \to 0$.

The Green's function giving the radiation to a far field point $\underset{\sim}{r}$ below the aircraft, due to a disturbance at $\underset{\sim}{Y}$ close to the slot, becomes:

$$G(\underset{\sim}{r},\underset{\sim}{y},t,\tau) = \frac{\phi_4^*(\underset{\sim}{Y})}{8\pi^2 r(1 - M\cos\theta)} \int_{-\infty}^{\infty} \frac{e^{i\omega[t]}\, d\omega}{\left[\frac{\pi i \chi}{2} - \ell n\left(\frac{\omega h \mu \sin\bar{\theta}}{2\pi c\sqrt{1 - M^2}}\right)\right]} . \qquad (A\text{-}44)$$

This expression may also be deduced from (A-36), (A-39) in the limit as $\omega\ell/c \to 0$ and when due account is taken of the change in the local potential functions $\phi_j^*(\underset{\sim}{Y})$ $(j = 1,3)$.

REFERENCES

Crighton, D.G.	1975	J. Fluid Mech. 72, 209-227. Scattering and diffraction of sound by moving bodies.
Fethney, P.	1975	An experimental study of airframe self-noise. AIAA 2nd Aeroacoustics Specialist's Conference. Hampton, Va, AIAA paper 75-511 (RAE Unpublished Material).
Ffowcs Williams, J.E.	1969	Ann. Rev. Fluid Mech. 1, 197-222. Hydrodynamic Noise.
Ffowcs Williams, J.E. Hall, L.H.	1970	J. Fluid Mech. 40, 657-670. Aerodynamic sound generation by turbulent flow in the vicinity of a scattering half-plane.
Ffowcs Williams, J.E. Lovely, D.J.	1976	J. Fluid Mech. 71, 689-700. Sound radiation into uniformly flowing fluid by compact surface vibration.
Gibson, J.S.	1972	The ultimate noise barrier - far field radiated aerodynamic noise. INTER-NOISE 72. Proc. Washington DC.
Gibson, J.S.	1973	Non-engine aerodynamic noise: the limit to aircraft noise reduction. INTER-NOISE 73, Proc. Copenhagen.
Gibson, J.S.	1974	Recent developments at the ultimate noise barrier. 9th Cong. Int. Counc. Aero. Sci., Haifa, Israel.
Hardin, J.C.	1976	Airframe self-noise - four years of research. NASA Tech. Memo. NASA TM X - 73908.
Healy, G.J.	1974	Measurement and analysis of aircraft far-field aerodynamic noise. CR - 2377 NASA.
Howe, M.S.	1975	J. Fluid Mech. 67, 597-610. The generation of sound by aerodynamic sources in an inhomogeneous steady flow.
Howe, M.S.	1976	J. Fluid Mech. 76, 711-740. The influence of vortex shedding on the generation of sound by convected turbulence.
Howe, M.S.	1977	J. Sound Vib. 50, 183-193. The effect of forward flight on the diffraction radiation of a high speed jet.
Kármán, T. von & Sears, W.R.	1938	J. Aero. Sci. 5, 379-390. Airfoil theory for non-uniform motion.

REFERENCES (concluded)

Lamb, H.	1932	Hydrodynamics 6th Ed. Cambridge University Press.
Morgan, H.G. & Hardin, J.C.	1974	Airframe Noise - the next aircraft noise barrier. AIAA Paper 74-949.
Rayleigh, Lord	1945	Theory of Sound, Vol II. Dover.
Stratton, J.A.	1941	Electromagnetic Theory. McGraw-Hill. New York.
Whittaker, E.T. & Watson, G.N.	1927	A Course of Modern Analysis. 4th Ed. Cambridge Univ. Press.

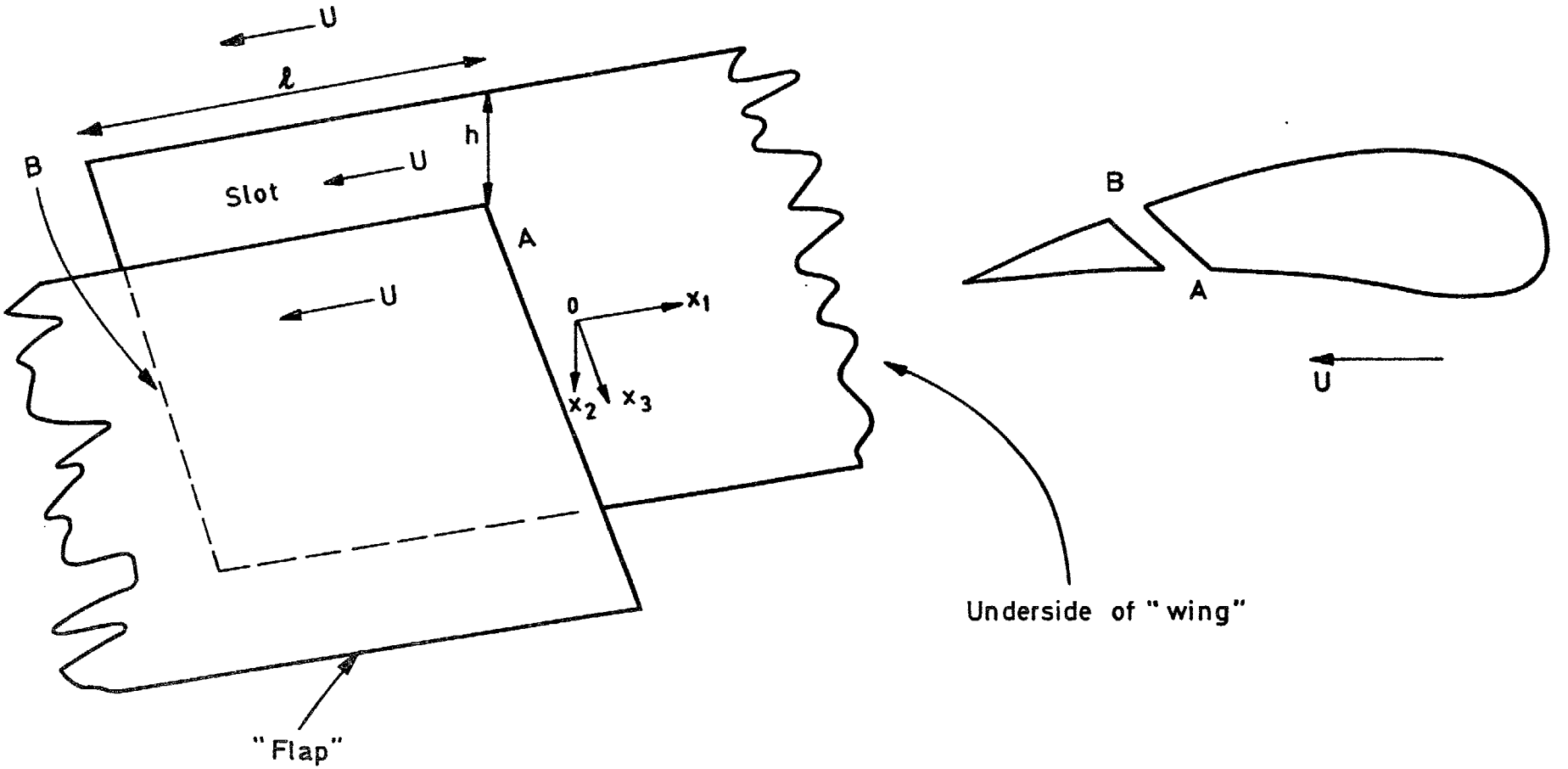

Fig 1a View from beneath the wing of slice through the semi-infinite, overlapping planes modelling the wing and flap. The overlap is of length ℓ and width h, and the ends A, B represent the openings A, B of the slot illustrated in an exaggerated manner in the accompanying sketch. The origin 0 of the x coordinate system lies on the underside of the wing in the plane of the mouth A. The x_1-axis is in the flight direction, x_2 perpendicular to the wing and vertically downwards, and x_3 parallel to the leading and trailing edges of the slot

Fig 1a

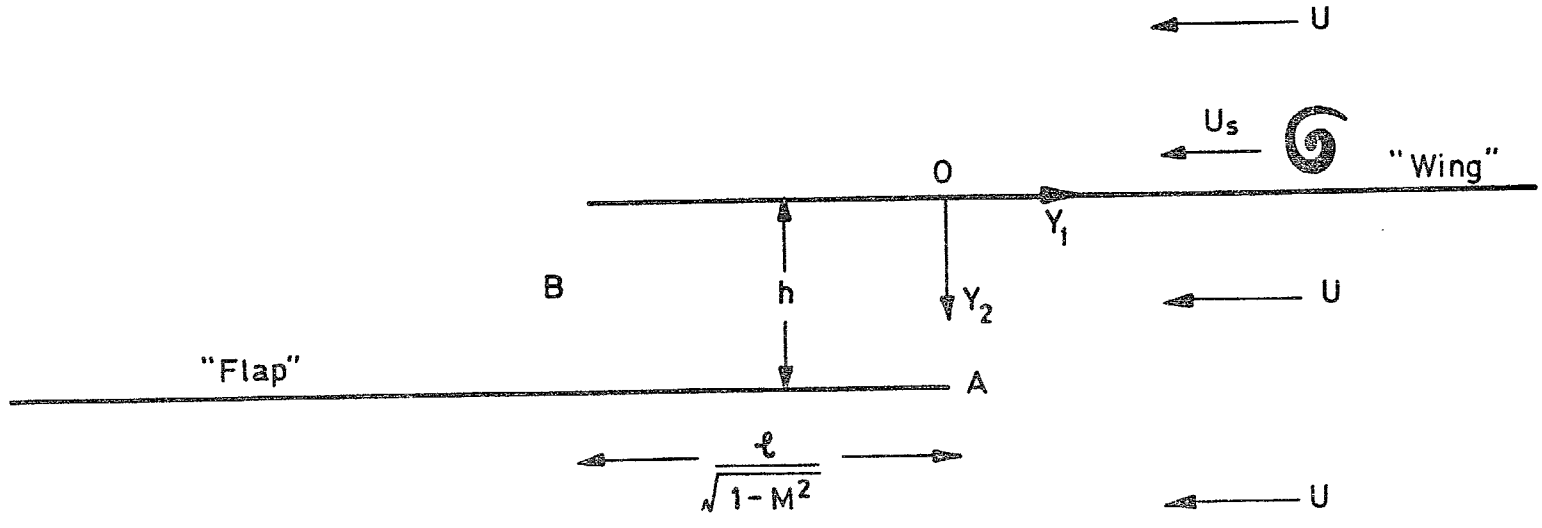

Fig 1b Illustrating the definition of the Prandtl-Glauert coordinate system $\underline{Y}$, in which $Z = Y_1 + iY_2$

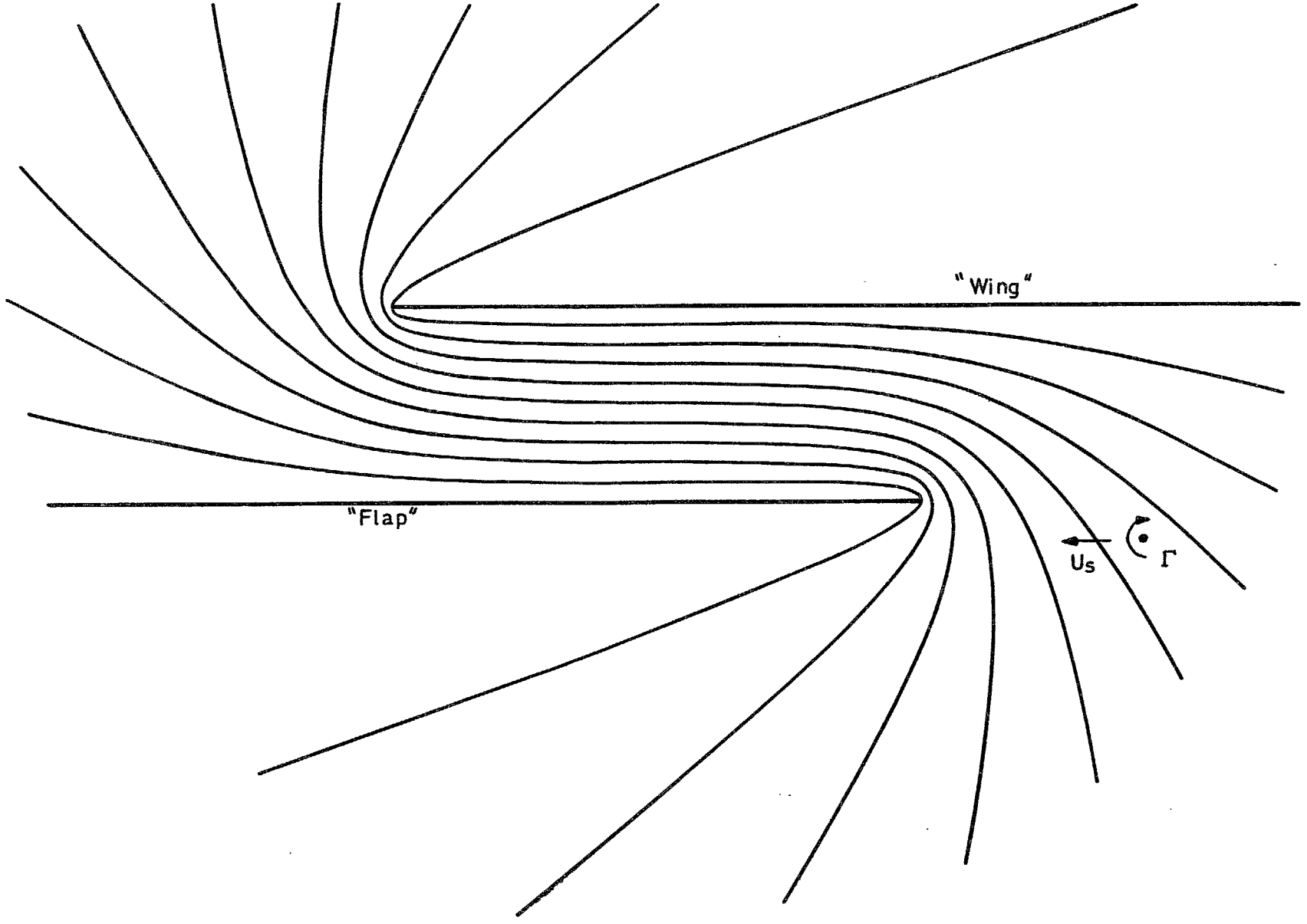

Fig 2 At very low frequencies the sound generated at the slot by a 'horse-shoe' vortex is determined by the degree to which the path followed by Γ, the transverse (ω_3-) component of vorticity, departs from one characterized by the streamlines of a two-dimensional potential flow through the slot for a fluid at rest at infinity

Fig 2

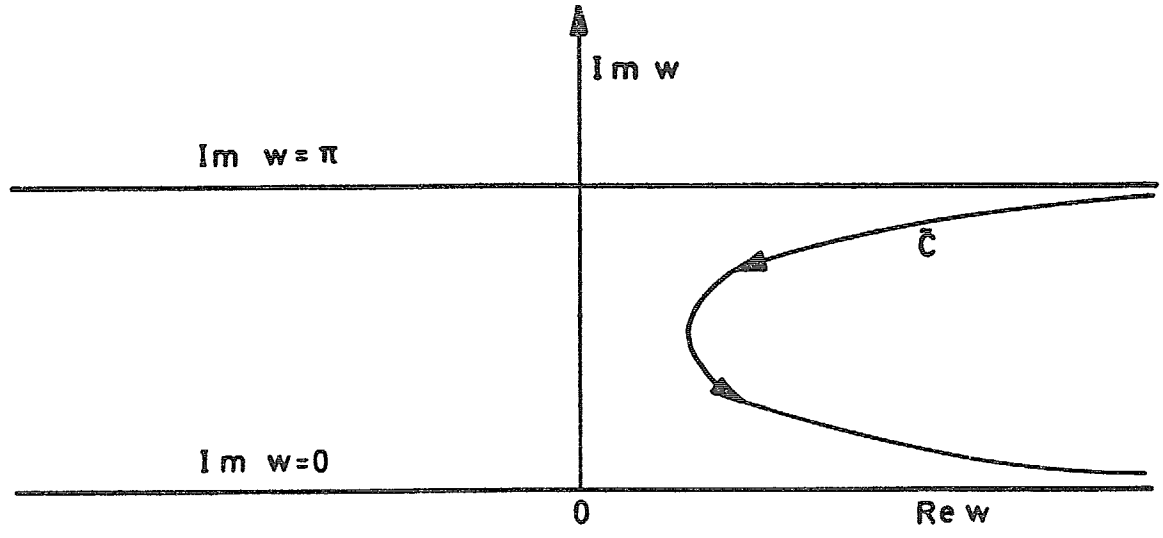

Fig 3 Path of integration in the w-plane for evaluating I_{11}

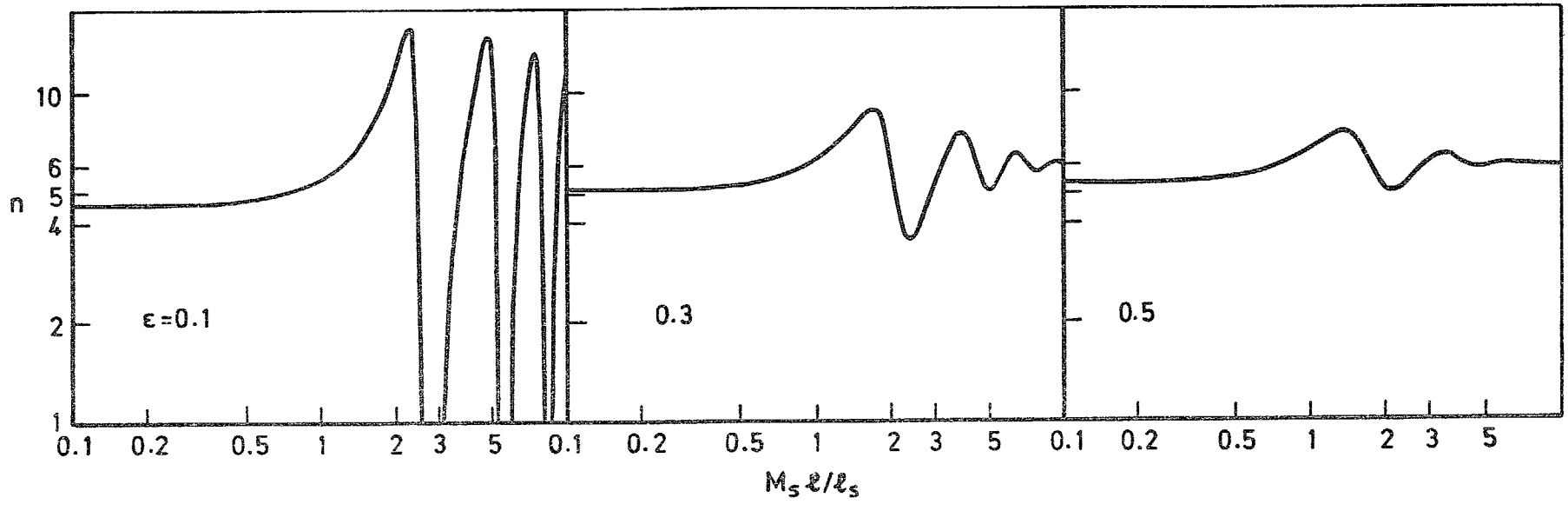

Fig 4 Variation of the velocity index n in the flyover plane as a function of $M_s\ell/\ell_s$ for three different values of $\epsilon = h/\ell$ in the case of over-the-wing turbulence with M = 0.2

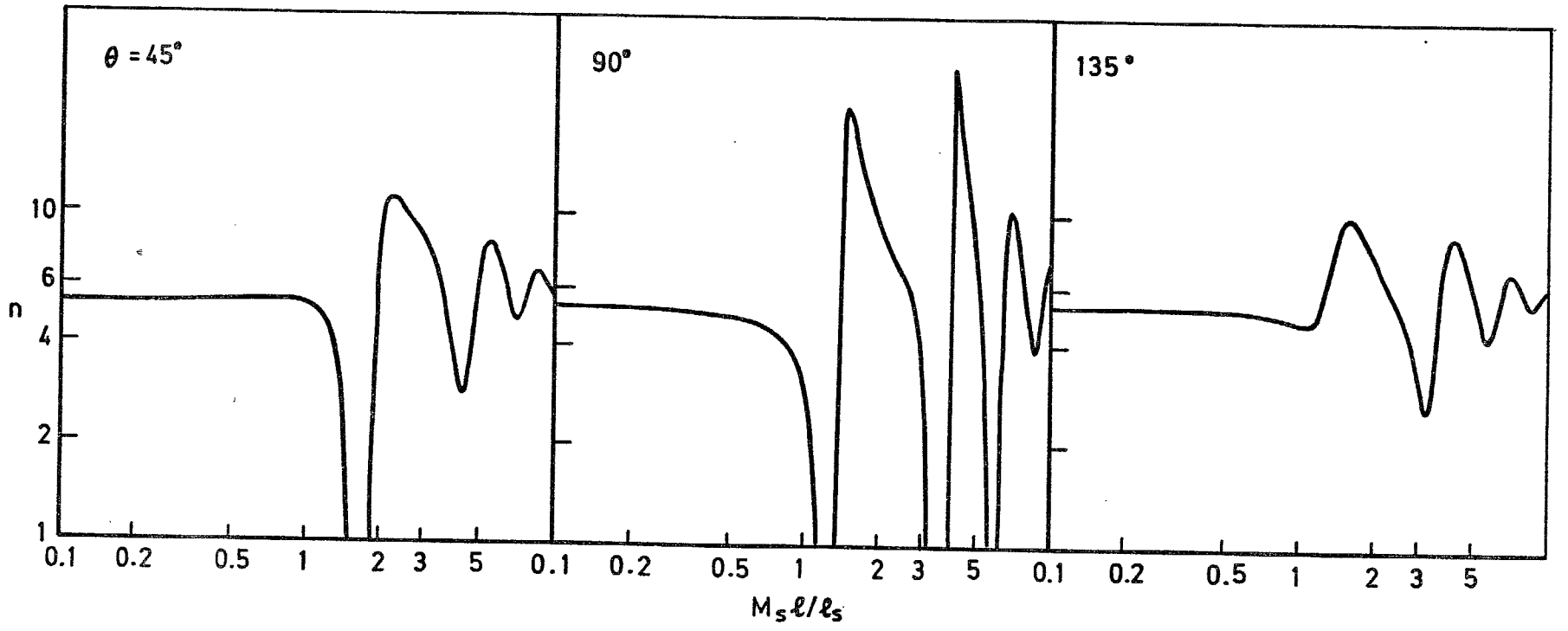

Fig 5 Variation of the velocity index n as a function of $M_s \ell/\ell_s$ for turbulence convecting below the wing and flap at M = 0.2, ϵ = 0.4 and for three directions in the flyover plane

Fig 6

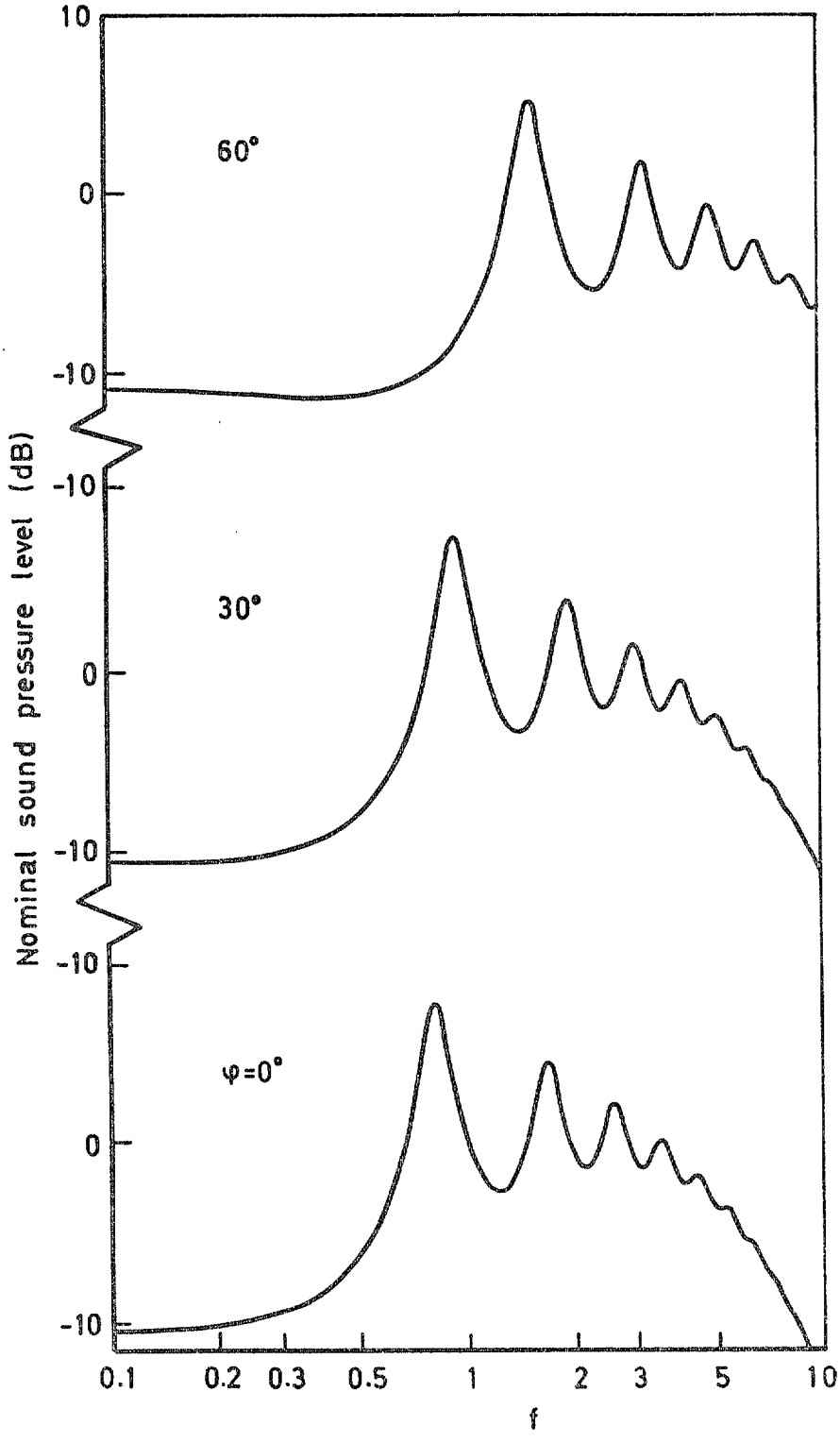

Fig 6 Illustrating the variation in the spectrum of sound

Printed in England for Her Majesty's Stationery Office by the Royal Aircraft Establishment, Farnborough. Dd. 586386 K4 12/78.

Published by
HER MAJESTY'S STATIONERY OFFICE

Government Bookshops
49 High Holborn, London WC1V 6HB
13a Castle Street, Edinburgh EH2 3AR
41 The Hayes, Cardiff CF1 1JW
Brazennose Street, Manchester M60 8AS
Southey House, Wine Street, Bristol BS1 2BQ
258 Broad Street, Birmingham B1 2HE
80 Chichester Street, Belfast BT1 4JY

Government Publications are also available through booksellers

R &M No.3830

ISBN 0 11 471163 1

HMSO